

X-ray crystal structure of tris(11-crown-3)triphenylene

Gerald W. Buchanan^{a,*}, Mastaneh Azad^a, Glenn P.A. Yap^b

^aDepartment of Chemistry, Ottawa Carleton Chemistry Institute, Carleton University, 1125 Colonel By Drive, Ottawa, Ont., Canada K1S 5B6.

^bDepartment of Chemistry, Ottawa-Carleton Chemistry Institute, University of Ottawa, Ottawa, Ont., Canada K1A 6N5.

Received 12 January 2001; accepted 26 March 2001

Abstract

Benzo-11-crown-3 ether trimerizes in the presence of FeCl_3 and aqueous H_2SO_4 to produce tris(11-crown-3)triphenylene. This compound crystallizes, along with a molecule of diethyl ether and CH_2Cl_2 in the triclinic $P\bar{1}$ space group; $a = 8.8913(9)$ Å, $b = 13.5790(14)$ Å, $c = 17.5244(17)$ Å, $\beta = 91.026(2)^\circ$, with $Z = 2$. Two of the three 11-crown-3 ether units of the trimer possess essentially identical geometries, while the third has a significantly different conformation. These stereochemical results are compared to those calculated for benzo-11-crown-3 in the gas phase. © 2001 Elsevier Science B.V. All rights reserved.

Keywords: Crown ether; Oxidative trimerization; Stereochemistry

1. Introduction

Hexaalkoxy-substituted triphenylenes show liquid-crystal properties if the side chains are of sufficient length. Hence, these molecules are important models for discotic liquid crystals [1,2]. A procedure for preparing 2,3,6,7,10,11-hexamethoxytriphenylene in near-quantitative yield was reported [3] using oxidative trimerization of 1,2-methoxybenzene, and recently we reported the application of this method to the synthesis of a novel tris(9-crown-3)triphenylene in ca. 25% yield [4].

We are interested in exploring the scope of this novel reaction to the synthesis and characterization of other tris(crown)triphenylene systems. Herein we report the synthesis of benzo-11-crown-3 ether **1** for the first time and its trimerization to tris(11-crown-3)-

triphenylene **2**. The single-crystal X-ray structure of **2** has been determined.

2. Results and discussion

In the presence of FeCl_3 and H_2SO_4 , **1** trimerizes in a low isolated yield (0.5%) to the triphenylene system **2** depicted in Fig. 1. Fig. 2 shows the ORTEP diagram for **2**. Table 1 contains selected atomic bond lengths and angles. Selected torsion angles involving non-hydrogen atoms are given in Table 2, while the crystallographic data are presented in Table 3. Atomic coordinates and equivalent isotropic displacement factors are given in Table 4. Anisotropic temperature factors are available as supplementary data as are structure factor tables.

2.1. X-ray crystal structure

With respect to bond lengths, there are significant differences found in the aryl C–O units, ranging from

* Corresponding author. Tel.: +1-613-520-3841; fax: +1-613-520-3749.

E-mail address: gwbuchan@ccs.carleton.ca (G.W. Buchanan).

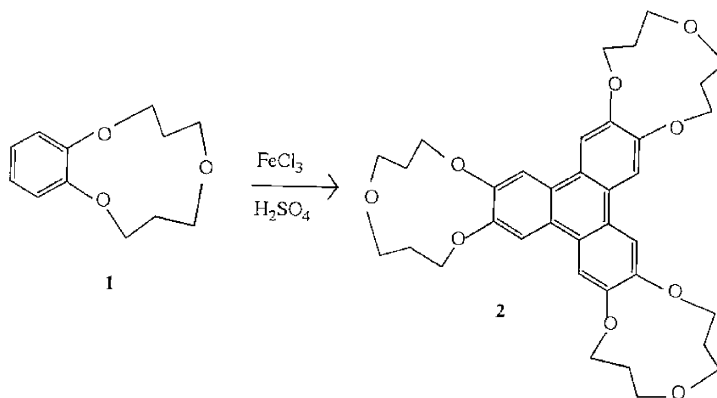


Fig. 1.

the shortest (1.361 Å) for C3–O1 to the longest (1.381 Å) for the C10–O3 moiety. A similar range of C–O bond lengths was noted for the related tris(9-crown-3)triphenylene studied previously [4]. A shorter C–O bond can be viewed as possessing more double bond character which should lead to a more deshielded ^{13}C resonance in the solid state spectrum. Indeed a range of ca. 5 ppm was found for the six aryl C–O resonances in tris(9-crown-3)

triphenylene in the ^{13}C CPMAS spectrum [4]. Unfortunately, the limited quantities of **2** available have precluded a solid state ^{13}C NMR investigation at this time.

In examining the bond angle data, it is clear that there are three anomalously large angles involving aromatic carbons and three correspondingly smaller angles involving the same central atoms. The central carbons involved are C3, C15 and C34. In the case of

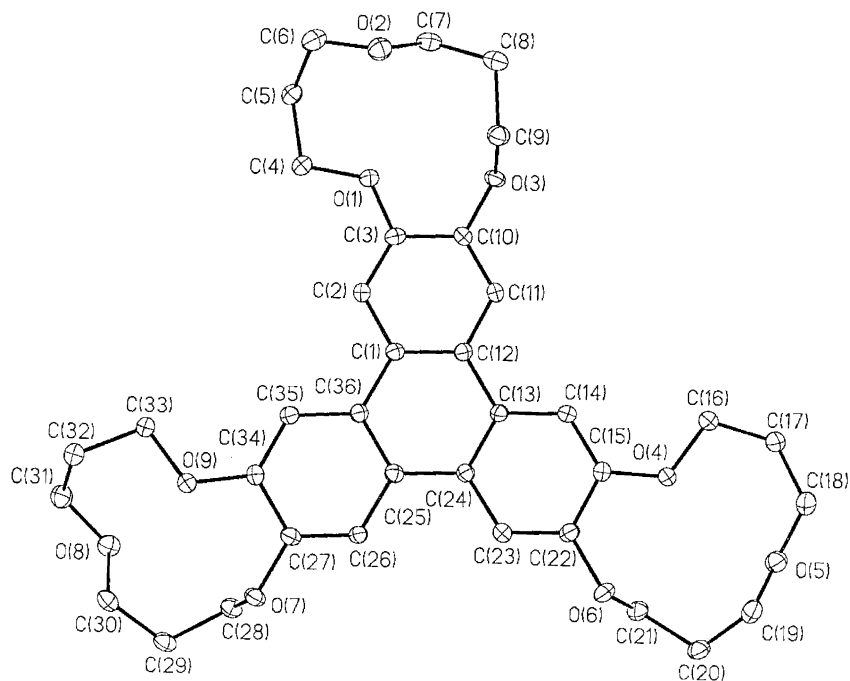


Fig. 2.

Table 1

(a) Atomic bond lengths (Å) and (b) selected atomic bond angles (°)

<i>Atomic bond lengths (Å)</i>					
O1–C3	1.361(3)	O1–C4	1.431(3)	O2–C6	1.418(3)
O2–C7	1.425(3)	O3–C10	1.381(3)	O3–C9	1.450(3)
O4–C15	1.364(3)	O4–C16	1.416(3)	O5–C19	1.419(3)
O5–C18	1.437(3)	O6–C22	1.378(3)	O6–C21	1.453(3)
O7–C27	1.383(3)	O7–C28	1.444(3)	O8–C31	1.428(3)
O8–C30	1.430(3)	O9–C34	1.365(3)	O9–C33	1.440(3)
C1–C12	1.412(3)	C1–C2	1.419(3)	C1–C36	1.466(3)
C5–C6	1.521(3)	C7–C8	1.513(3)	C8–C9	1.517(3)
C10–C11	1.364(3)	C11–C12	1.409(3)	C12–C13	1.469(3)
C13–C24	1.405(3)	C13–C14	1.408(3)	C14–C15	1.377(3)
C15–C22	1.405(3)	C16–C17	1.513(3)	C17–C18	1.514(4)
C19–C20	1.511(3)	C20–C21	1.507(3)	C22–C23	1.370(3)
C23–C24	1.410(3)	C24–C25	1.460(3)	C25–C26	1.411(3)
C25–C36	1.411(3)	C26–C27	1.364(3)	C27–C34	1.410(3)
C28–C29	1.510(3)	C29–C30	1.508(3)	C31–C32	1.520(3)
C32–C33	1.505(3)	C34–C35	1.369(3)	C35–C36	1.414(3)
<i>(b) Selected atomic bond angles (°)</i>					
C3–O1–C4	120.2(2)	C6–O2–C7	114.6(2)		
C10–O3–C9	112.1(2)	C15–O4–C16	120.6(2)		
C19–O5–C18	115.1(2)	C22–O6–C21	116.3(2)		
C27–O7–C28	112.3(2)	C31–O8–C30	114.4(2)		
C34–O9–C33	119.5(2)	O1–C3–C2	126.4(2)		
O1–C3–C10	113.8(2)	O1–C4–C5	105.6(2)		
C4–C5–C6	114.5(2)	O2–C6–C5	115.5(2)		
O2–C7–C8	108.5(2)	C7–C8–C9	113.0(2)		
C8–C9–O3	110.9(2)	C11–C10–O3	121.5(2)		
C3–C10–O3	119.0(2)	O4–C15–C14	125.2(2)		
O4–C15–C22	115.2(2)	O4–C16–C17	107.4(2)		
C16–C17–C18	114.3(2)	O5–C18–C17	110.4(2)		
O5–C19–C20	109.2(2)	C19–C20–C21	114.1(2)		
O6–C21–C20	107.7(2)	C23–C22–O6	119.1(2)		
O6–C22–C15	121.1(2)	O7–C27–C34	119.2(2)		
O7–C28–C29	111.4(2)	C30–C29–C28	114.5(2)		
O8–C30–C29	107.4(2)	O8–C31–C32	115.2(2)		
O9–C33–C32	106.0(2)	O9–C34–C35	126.1(2)		
O9–C34–C27	113.9(2)				

C3, the O1–C3–C2 angle is found to be 126.4°, which is ca. 6° larger than expected for an sp² hybridized centre. It appears that the O1–C3–C2 angle ‘opens up’ in an attempt to minimize the effect of the steric repulsion resulting from the nearly coplanar ($\theta = 17.3^\circ$) torsional C4–O1–C3–C2 unit. Such an expansion does not occur in the O3–C10–C11 unit since the torsion angle for the C9–O3–C10–C11 network is -102.7° . The expansion of the O1–C3–C2 bond angle is accompanied by a contraction of the O1–C3–C10 angle to 113.8° with the ‘internal’ C2–C3–C10 angle having a normal value of ca. 120°.

At C15, we attribute the anomalously large (125.2°) O4–C15–C14 angle to the same factors as described before for C3, since the C14–C15–O4–C16 torsion angle is 14.7°. Similarly at C34, the expansion of the O9–C34–C35 angle to 126.1° can be attributed to the repulsive torsional interactions arising from the nearly coplanar ($\theta = 16.7^\circ$) C33–O9–C34–C35 network.

With respect to the conformation of the 11-membered rings in **2**, there are no reports in the literature of any 11-crown-3 systems. A comparison of torsion angles for the 11-membered rings is presented in Table 5 and it is evident that two of the three

Table 2
Selected torsion angles (°)

C4–O1–C3–C2	17.3(3)	C4–O1–C3–C10	– 163.0(3)
C1–C2–C3–O1	177.5(2)	O1–C4–C5–C6	– 77.3(2)
C3–O1–C4–C5	174.8(2)	C7–O2–C6–C5	68.1(3)
C4–C5–C6–O2	49.3(3)	C6–O2–C7–C8	– 173.3(2)
O2–C7–C8–C9	60.2(3)	C10–O3–C9–C8	– 146.6(2)
C7–C8–C9–O3	71.3(2)	C9–O3–C10–C11	– 102.7(3)
C9–O3–C10–C3	78.4(2)	O1–C3–C10–C11	– 175.2(2)
O3–C10–C11–C12	178.6(2)	C11–C12–C13–C14	– 2.8(2)
C16–O4–C15–C14	14.7(4)	C16–O4–C15–C22	– 164.7(2)
C13–C14–C15–O4	– 179.6(2)	C15–O4–C16–C17	– 174.5(3)
O4–C16–C17–C18	– 50.2(3)	C19–O5–C18–C17	– 129.5(3)
C16–C17–C18–O5	81.6(3)	C18–O5–C19–C20	156.2(2)
O5–C19–C20–C21	– 68.7(3)	C22–O6–C21–C20	148.6(2)
C19–C20–C21–O6	63.4(3)	C21–O6–C22–C23	120.8(2)
C21–O6–C22–C15	– 65.1(3)	C28–O7–C27–C26	– 101.5(2)
C28–O7–C27–C34	79.4(2)	C27–O7–C28–C29	– 144.3(2)
O7–C28–C29–C30	69.7(3)	C31–O8–C30–C29	– 173.9(2)
C28–C29–C30–O8	60.4(3)	C30–O8–C31–C32	68.2(3)
O8–C31–C32–C33	48.8(3)	C34–O9–C33–C32	173.1(2)
C31–C32–C33–O9	– 75.7(3)	C33–O9–C34–C35	16.7(3)
C33–O9–C34–C27	– 163.1(2)		

Table 3
Crystallographic data for **2**

Formula	C ₄₁ H ₁₀ O ₁₀
Formula weight (g/mol)	777.74
Temperature (K)	203(2)
Crystal system	triclinic
Space group	<i>P</i> -1
<i>a</i> (Å)	8.8913(9)
<i>b</i> (Å)	13.5790(14)
<i>c</i> (Å)	17.5244(17)
β (°)	91.026(2)
Volume (Å ³)	1909.6(3)
<i>Z</i> (molecules per unit cell)	2
<i>D_c</i> (gm/cm ³)	1.353
Crystal dimensions (mm ³)	0.2 × 0.1 × 0.1
Radiation (λ , Å)	MoK α , 0.71073
Octants measured	<i>h</i> (–11 to 11), <i>k</i> (–18 to 17), <i>l</i> (–22 to 17)
Theta range (°)	1.66 to 28.68
No. of unique reflections	8624
No. of reflections measured	14,943
No. of reflections with <i>I</i> > 2 σ (<i>I</i>)	7724
<i>R</i> ₁ (<i>I</i> > 2 σ (<i>I</i>))	0.0547
<i>R</i> ₁ (all data)	0.0998
<i>wR</i> ₂ (all data)	0.1491
<i>wR</i> ₂ (<i>I</i> > 2 σ (<i>I</i>))	0.1343
GoF	1.04
Largest diff. peak and hole (e Å ^{–3})	0.600 and –0.680

11-membered rings of **2** have essentially the same geometries, while the third (C15–C22) has a unique conformation. Unfortunately, benzo-11-crown-3,1, is an oil, however we have used the HyperChem program to calculate the preferred geometry of the 11-membered ring of **1** in the gas phase. These data are included in Table 5 for comparison. It is important to include H atoms in the HyperChem structure of **1** and a fair agreement between observed solid state geometries and the calculated gas phase structure for the 11-membered ring of **1** is found. When viewing the ORTEP plot of **2** (Fig. 2), it is clear that there is a ‘northern’ ring (i.e. C3–C10), an ‘eastern’ ring (i.e. C15–C22) and a ‘western’ ring (C27–C34). The northern and western rings have identical conformations. The primary differences between the conformation of the eastern ring and the other two crown units are in the region most remote from the central core of the molecule-i.e. in the C5–C6–O2–C7–C8 region, where differences in torsion angles up to ca. 60° are found.

Conversely, the calculations for **1** in the gas phase show the largest differences in torsion angles from those found in **2** in the region surrounding the site corresponding to O1 in **1**. Of course, crystal packing effects limit the value of detailed comparisons

Table 4

Atomic coordinates ($\times 10^4$) and equivalent isotropic displacement parameters ($\text{\AA}^2 \times 10^3$). $U(\text{eq})$ is defined as one third of the trace of the orthogonalized U_{ij} tensor

	<i>x</i>	<i>y</i>	<i>z</i>	<i>U</i> (eq)
O1	4517(2)	− 1156(1)	1070(1)	35(1)
O2	4380(2)	− 2919(1)	1611(1)	36(1)
O3	4238(2)	− 51(1)	2625(1)	29(1)
O4	8207(2)	5573(1)	4580(1)	41(1)
O5	9090(2)	7656(1)	5839(1)	35(1)
O6	10513(2)	6404(1)	3844(1)	36(1)
O7	11755(2)	3436(1)	− 227(1)	29(1)
O8	10255(2)	1777(1)	− 2386(1)	35(1)
O9	10504(1)	1322(1)	− 936(1)	35(1)
C1	7378(2)	1443(2)	1391(2)	24(1)
C2	6508(3)	348(2)	998(1)	27(1)
C3	5450(2)	− 129(2)	1395(1)	28(1)
C4	4862(3)	− 1949(2)	336(2)	33(1)
C5	3688(3)	− 3008(2)	202(2)	33(1)
C6	4038(2)	− 3584(2)	759(2)	39(1)
C7	3103(3)	− 2549(2)	1999(2)	37(1)
C8	3685(3)	− 1747(2)	2871(2)	37(1)
C9	4912(3)	− 758(2)	2904(2)	33(1)
C10	5249(2)	461(2)	2220(1)	25(1)
C11	6033(2)	1527(2)	2597(1)	26(1)
C12	7093(2)	2054(2)	2198(1)	24(1)
C13	7907(2)	3208(2)	2612(1)	24(1)
C14	7606(3)	3839(2)	3406(1)	29(1)
C15	8416(3)	4906(2)	3810(1)	31(1)
C16	7368(3)	5137(2)	5110(2)	35(1)
C17	7213(3)	6088(2)	5872(2)	39(1)
C18	8723(3)	6923(2)	6264(2)	42(1)
C19	10612(3)	7798(2)	5600(2)	36(1)
C20	10640(3)	8165(2)	4882(2)	35(1)
C21	9758(3)	7305(2)	4092(2)	35(1)
C22	9569(3)	5379(2)	3426(1)	29(1)
C23	9856(3)	4775(2)	2648(1)	29(1)
C24	9025(2)	3687(2)	2214(1)	24(1)
C25	9331(2)	3056(2)	1382(1)	25(1)
C26	10396(2)	3536(2)	957(1)	25(1)
C27	10722(2)	2953(2)	186(1)	27(1)
C28	10979(3)	3677(2)	− 845(1)	31(1)
C29	11859(3)	3519(2)	− 1593(2)	34(1)
C30	11837(3)	2346(2)	− 2104(2)	33(1)
C31	10020(3)	626(2)	− 2812(2)	39(1)
C32	10342(3)	11(2)	− 2281(2)	35(1)
C33	9599(3)	272(2)	− 1488(1)	33(1)
C34	10009(3)	1830(2)	− 192(1)	27(1)
C35	8925(3)	1350(2)	190(1)	27(1)
C36	8544(2)	1949(2)	980(1)	24(1)

between gas phase calculations and experimental X-ray data.

The four aromatic rings of **2** are essentially coplanar, in contrast to the situation for tris(9-crown-3)triphenylene [4] where deviations from coplanarity up to ca. 14° were found.

2.2. ^{13}C NMR spectra

The solution ^{13}C spectrum (CDCl_3 solvent) contains only six resonances, as expected from the three-fold symmetry element present in the planar depiction of **2**, which arises from sufficiently rapid conformational interconversions at room temperature.

3. Experimental

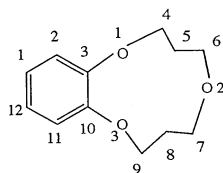
3.1. Materials

The synthetic sequence leading to **2** begins with the synthesis of the previously unknown benzo-11-crown-3 ether, **1**. Preparation of **1** was carried out starting with 3-chloropropanol (Aldrich) which was subsequently converted to 1,7-dichloro-4-oxaheptane via the following method.

A 250 ml round-bottom flask was charged with 3-chloropropanol (100.0 g, 1.1 mol) and the flask was fitted with a condenser and a dropping funnel. To this was added drop wise with stirring, concentrated H_2SO_4 (70 ml) and the reaction mixture was refluxed overnight. After cooling, the mixture was poured onto ice (300 g), neutralized with 3 M NaOH and extracted with CH_2Cl_2 (4×300 ml). The combined organic layers were dried over anhydrous sodium sulfate and the drying agent was removed by filtration. The solvent was removed via *roto* evaporation to yield 39.5 g of crude 1,7-dichloro-4-oxaheptane, as a dark green oil, which was used without further purification in the next step.

For preparation of **1**, a three-necked 3 l round bottom flask, equipped with a dropping funnel and condenser, was charged with catechol (Aldrich, 25.0 g, 0.23 mol), distilled water (2.5 l) and $\text{LiOH} \cdot 2\text{H}_2\text{O}$ (20.0 g, 0.48 mol). This mixture was then stirred under reflux for 1 h. Subsequently 1,7-dichloro-4-oxaheptane (38.9 g, 0.23 mol) was added drop wise with stirring and the mixture was refluxed for 5 days. After cooling, the mixture was acidified to

Table 5

Comparison of calculated 11-membered ring torsion angles (°) in **1** with those in the crystal structure of **2**

Network	1	C3–C10 (2)	C15–C22 (2)	C27–C34 (2)
C3–C10–O3–C9	61.4	78.4	– 65.1	79.4
C10–O3–C9–C8	– 148.7	– 146.6	148.6	– 144.3
O3–C9–C8–C7	98.7	71.3	63.4	69.7
C9–C8–C7–O2	– 85.9	60.2	– 68.7	60.4
C8–C7–O2–C6	161.1	– 173.3	156.2	– 173.9
C7–O2–C6–C5	– 74.3	68.1	– 129.5	68.2
O2–C6–C5–C4	– 50.1	49.3	81.6	48.8
C6–C5–C4–O1	100.6	– 77.3	– 50.2	– 75.7
C5–C4–O1–C3	– 166.6	174.8	– 174.5	173.1
C4–O1–C3–C10	109.5	– 163.0	– 164.7	– 163.1
O1–C3–C10–O3	– 10.9	3.7	6.4	3.2

pH 3 using concentrated H_2SO_4 and then extracted with CH_2Cl_2 (3×300 ml). The combined organic layers were washed with 5% NaOH (3×300 ml) and water (2×200 ml) and dried over anhydrous sodium sulfate. Rotary evaporation yielded an oil, which was then treated with boiling hexane (5×300 ml). The hexane extracts were decanted into a beaker, whereupon a small quantity (0.8 g) of white crystals precipitated. This material was removed by filtration and subsequently identified as dibenzo-22-crown-6 ether. The hexane filtrate was concentrated by rotary evaporation to yield a dark yellow oil. This oil was subjected to column chromatography on silica gel using CH_2Cl_2 : diethyl ether (95:5) as eluent and yielded 9.0 g (19.2%) of benzo-11-crown-3 ether **1**, as a pale yellow oil, which was identified by ^{13}C NMR (CDCl_3 solvent) with resonances at 29.4, 66.4, 69.5, 118.4, 122.6 and 150.9 ppm. High-resolution mass spectrum: calculated m/e 208.2573, observed 208.1085.

For the preparation of **2**, a 500 ml double-necked round bottom flask was equipped with a dropping funnel and a condenser with a gas inlet tube. To a mixture of FeCl_3 (10.5 g, 0.065 mol), CCl_4 (120 ml) and concentrated H_2SO_4 (0.75 ml) in this flask was added **1**, (4.5 g, 0.022 mol) drop wise with vigorous

stirring under N_2 . Reflux was carried out for 4 days. Then 120 ml of methanol was added and the mixture was refluxed for one more day. After cooling, 100 ml of distilled water was added and the crude product was extracted with CH_2Cl_2 (3×200 ml). The combined organic layers were dried over anhydrous Na_2SO_4 and the solvent was removed by rotary evaporation to yield 4.0 g of a dark brown oil. ^1H NMR indicated that this was a mixture of **1** and **2** in a ratio of ca. 8:1.

The dark brown oil was boiled in hexane (5×400 ml) to dissolve the unreacted **1** and a brown precipitate resulted. This precipitate was collected by vacuum filtration and washed with a further 300 ml of hot hexane. Subsequently, the resulting brown powder was transferred to a beaker and 30 ml of acetone was added to produce a light yellow precipitate. This light yellow solid was then dissolved in 40 ml of CH_2Cl_2 and boiled with activated charcoal. After gravity filtration, the volume of solution was reduced to ca. 10 ml by boiling and then anhydrous diethyl ether (20 ml) was added. After 3 days, 0.007 g (0.5% yield) of **2**, mp $285\text{--}290^\circ\text{C}$ were obtained as light yellow needles. ^{13}C NMR (CDCl_3): 150.4, 124.9, 111.6, 69.8, 66.5 and 29.6 ppm. Mass spectrum ($M + 1$) $m/z = 619$.

The low isolated yield of **2**, (0.5%) is most likely due to the difficulty in freeing the trimeric material from its complex with FeCl₃. The crude yield is estimated to be ca. 12% based on the above mentioned ¹H NMR integration results.

3.2. ¹³C NMR spectra

¹³C solution spectra were recorded at 100.6 MHz using a Bruker AMX 400 instrument with complete ¹H noise decoupling. An Aspect 3000 processing controller was employed and all standard micro programs used are in the Bruker Software Library.

3.3. X-ray crystallographic studies and structure refinement

Suitable crystals were selected and mounted on thin glass fibres using viscous oil. Data were collected on a Bruker AX SMART 1k CCD diffractometer using 0.3° scans at 0, 90 and 180°. Unit cell parameters were determined from 60 data frames collected at different sections of the Ewald sphere. Semi-empirical absorption corrections based on equivalent reflections were applied [5].

Unit cell parameters and systematic absences in the diffraction data are consistent with the space group *P* $\bar{1}$. The structure was solved by direct methods,

completed with difference Fourier syntheses and refined with full-matrix least-squares procedures based on F². All non-hydrogen atoms were refined with anisotropic displacement parameters and hydrogen atoms were treated as idealized contributions. All scattering factors and anomalous dispersion factors are contained in the SHEXTL 5.1 program library.

Acknowledgements

G.W. Buchanan thanks the Natural Sciences and Engineering Research Council of Canada (NSERC) for continued financial support via Research Grants. We also thank Majid Rastegar for his invaluable assistance in this work.

References

- [1] A.M. Levelut, J. Chim. Phys. 80 (1983) 149.
- [2] S. Chandrasekhar, G.S. Ranganath, Rep. Prog. Phys. 53 (1990) 57.
- [3] H. Naarmann, M. Hanack, R. Mattmer, Synthesis 477 (1994).
- [4] G.W. Buchanan, M.F. Rastegar, G.P.A. Yap, Can. J. Chem. (2001).
- [5] R. Blessing, Acta Crystallogr. A51 (1995) 33.